DYNAMIC CHARACTERISTICS AND WIND INDUCED RESPONSE OF A STEEL FRAME TOWER

M.J.Glanville and K.C.S.Kwok

The University of Sydney
School of Civil & Mining Engineering

Abstract: *This paper describes a field measurement program being conducted on a steel frame tower. Dynamic characteristics of the tower are measured to determine its frequencies of vibration, mode shapes and damping values. A STRAND6 computer model is assembled and confirms these findings. Finally the dynamic response of the tower under wind loading is investigated.*

1. Introduction

A microwave communications tower was constructed in 1992 at Prospect County Council in the western suburbs of Sydney. The 67m high tower had to satisfy strict deflection limits for both static and dynamic loads to reduce signal transmission interference and loss. This was achieved using a frame system comprising of four circular column sections rigidly joined to rolled section platforms.

The Prospect tower was chosen for investigation because of its conservative design to wind loading. Testing commenced in June 1992 before any microwave dishes were installed on the tower in order to fully understand the wind induced response and dynamic characteristics of this stiff structure.

2. Measurement Program

Two accelerometers are installed at the 57m level and aligned orthogonally along the tower's major axes. Wind speed and direction are measured at the same level using a cup anemometer and wind vane respectively. Analogue data is transmitted via co-axial cable to the base of the tower where it is recorded onto magnetic tape and later converted into digital format. Wind with yaw angle between 20° and 100° (see Figure1) is not recorded to avoid interference from the tower.

Force vibration tests were performed on the tower in order to obtain decay curves for each mode of vibration. The tower was excited into vibration by oscillating a body weight in time with a metronome at each natural frequency of the tower. Forcing ceased once the tower was resonating at which time the tower was allowed to vibrate freely until it came to rest. Force vibration tests were performed during still atmospheric conditions to eliminate any background excitation.

Tower decay during force excitations was measured using the installed accelerometers and a laser beam. A He-Ne laser was placed at the base of the tower and magnified through a zenith plummet. The beam was projected onto a grid placed at the top of the tower. The relative movement of the grid to the stationary beam was then filmed for later analysis.

Mode shape of the tower was measured using an additional set of accelerometers. After calibration at the 57m level of the tower, one pair of accelerometers was moved step by step to lower levels. Mode shape was determined from the ratio of simultaneously recorded acceleration signals. The presence of any torsional modes was similarly detected using an additional pair of accelerometers eccentrically placed at the 57m level.

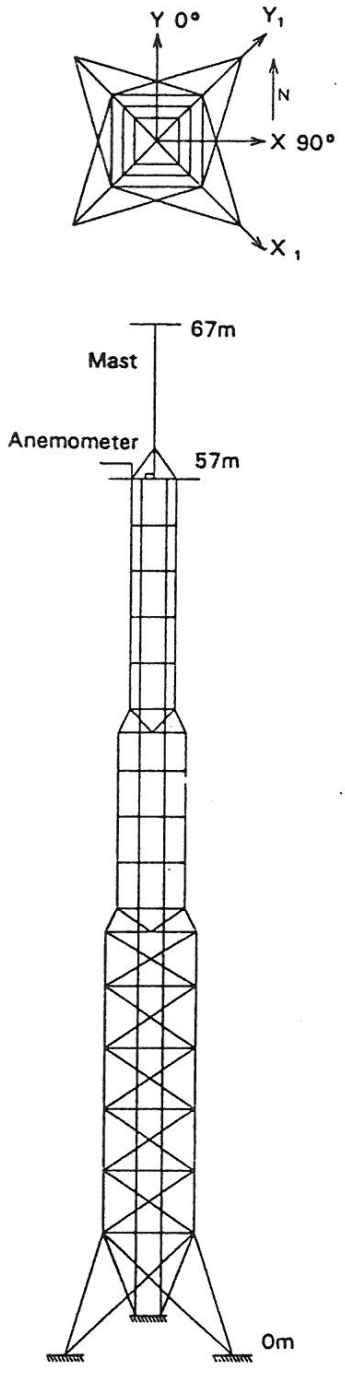

Figure 1 General arrangement of the Prospect tower.

3. Computer Model

Natural frequencies and mode shapes for the tower were calculated using STRAND6. STRAND6 is a commercially available suite of full three dimensional finite element programs including a natural frequency solver. The natural frequency solver calculates the natural frequencies (eigenvalues λ) and vibration modes (eigenvectors {x}) based on a lumped mass assumption and solving the equation:

$$[K]\{x\} = \lambda [M]\{x\}$$

[K] and [M] represent the banded stiffness matrix and the lumped (diagonal) mass matrix respectively.

4. Results

4.1 Dynamic Characteristics

4.1.1 Natural Frequency

Power Spectral Density was computed for the acceleration response of the tower under wind loading (Figure2). Spectral peaks indicate that mode one dominates the tower's response at 1.08Hz. The two smaller peaks represent the second and third modes of tower vibration. The difference in natural frequencies along perpendicular axes are less than 2% producing strong coupling between the X-X and Y-Y axis.

Natural frequency values obtained through full scale measurement are compared to those calculated by STRAND6 in Table1. The computed results agree well with those measured, particularly modes one and two.

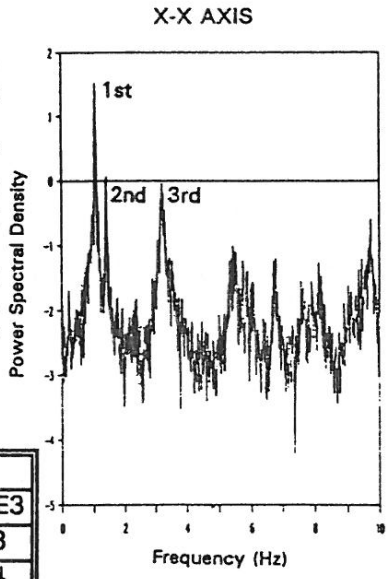

Figure 2 Power spectra of acceleration

Table 1

NATURAL FREQUENCY	X-X AXIS (Hz)			Y-Y AXIS (Hz)		
	MODE 1	MODE 2	MODE 3	MODE 1	MODE2	MODE3
FULL SCALE	1.08	1.41	3.22	1.07	1.39	3.28
STRAND6	1.10	1.40	3.52	1.10	1.40	3.54
STRAND6-MAST	1.14	3.53	6.06	1.14	3.54	6.07

4.1.2 Mode Shape

The mode shapes measured in full scale are compared to those calculated by STRAND6 in Figure3. Figure4 is a STRAND6 three dimensional representation of mode one vibrating along the Y-Y axis.

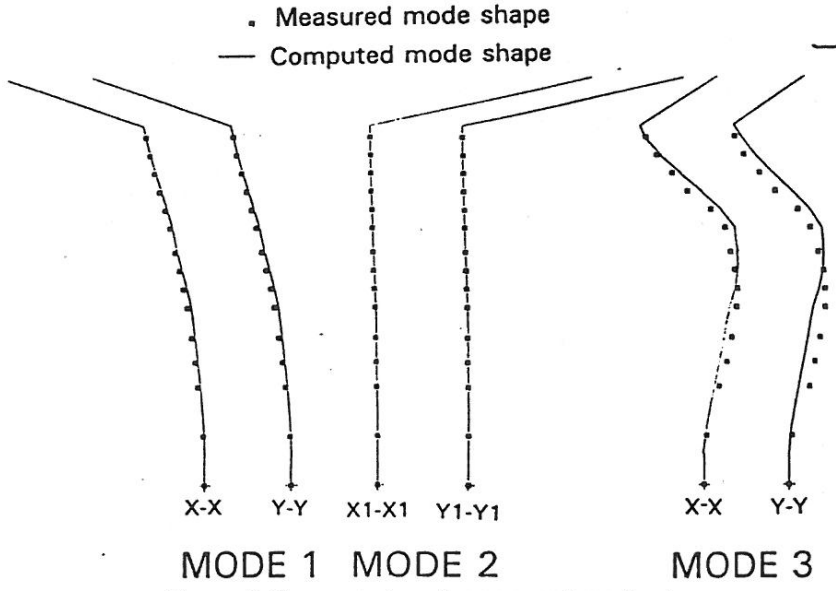

Figure 3 Computed and measured mode shapes

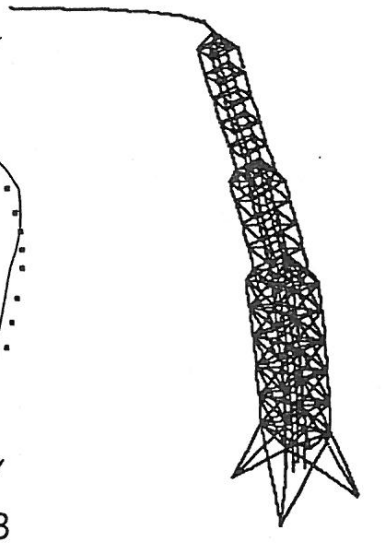

Figure 4 Mode 1 Y-Y axis

Mode one displays typical quarter sine wave bending with the top mast dominating the tower's displacement. The ratio of mast displacement to tower displacement is about 2.5:1. The ratio of mast to tower displacement in mode two is about 24:1 suggesting that this mode of vibration is due to the vibration of the top mast alone. Mode three displays the full sine wave shape with a small amount of torsion towards the top of the tower. Some torsion was measured in full scale at mode three only. Two eccentrically placed angle sections running up one side of the top third of the tower are probably responsible for this behaviour. It should be noted that a purely torsional mode was calculated by STRAND6 at 2.7Hz however no evidence of this mode was found during full scale measurement.

STRAND6 was used to simulate removal of the top mast from the tower. Table1 summarises the new frequencies found after the mast was removed. The natural frequency and mode shape of mode two without the mast is almost identical to that of mode three before the mast was removed as shown in Figure3. The natural frequency of the mast removed from the tower was also calculated by STRAND6 at 1.4Hz. This confirms that the second mode of the tower is simply the natural frequency of the top mast. Removing the mast would remove this mode of vibration.

4.1.3 Damping

High amplitude free vibration decay curves obtained from filtered acceleration records for mode one are shown in Figure5. Percentage critical damping along the Y-Y axis is greater than that along the X-X axis. This may be attributed to the higher number of bolted connections which offer additional damping along the Y-Y axis. Alignment of the tower's ladders and cable trays running up the centre of the tower also contribute to the higher value of damping. Damping for modes two and three was similarly determined at 0.25% critical damping and 1.5% critical damping respectively. A low value of damping at mode two is expected since this mode represents vibration of the mast alone.

The decay curves shown in Figure5 are peculiar since they exhibit lower damping at higher amplitudes. This may be explained by the large dependence of mode one upon the vibration of the lightly damped mast which acts as an excitation mechanism during tower decay. It is intended to guy the mast in full scale and repeat the free vibration tests to confirm this.

Figure6 is a plot of the peak tower displacements as mapped from the laser trace during a free vibration decay along the tower's X-X axis. Both methods of decay analysis produce the same damping values as expected.

An autocorrelation analysis was employed to measure tower damping at relatively low amplitudes

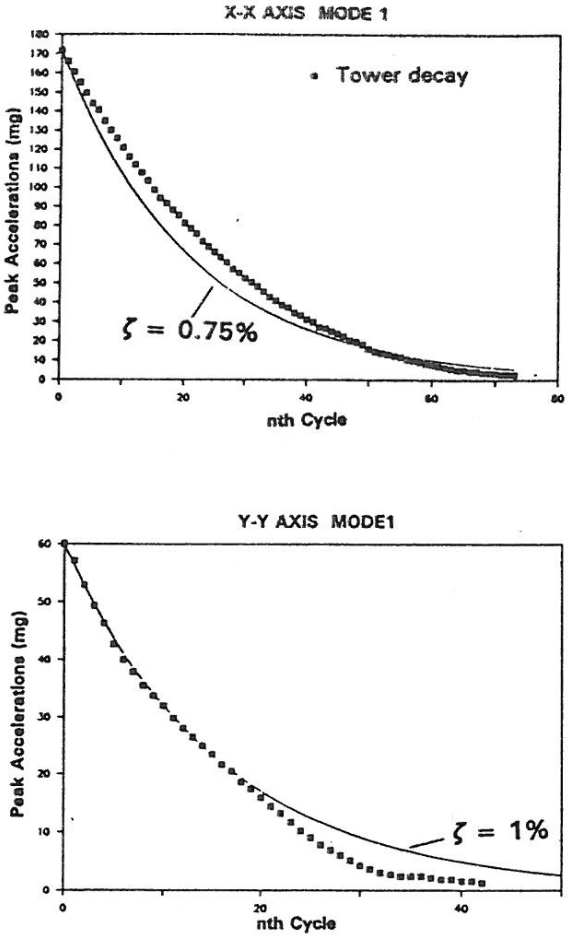

Figure 5 Free vibration decay curves obtained from acceleration records.

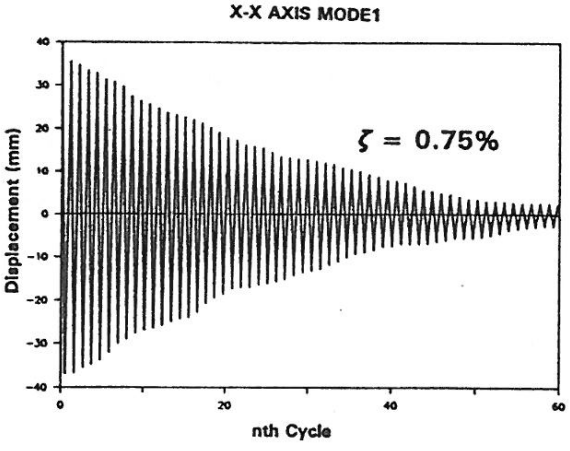

Figure 6 Free vibration decay mapped from laser trace

under wind loading alone (less than 5mg). One of the requirements for an autocorrelation analysis to be stable statistically is stationarity of the data on which the analysis is based. Jeary (ref 4) describes the run test for stationarity based on the variation of rms response. Figure7 presents the results of such a run test performed on a sample of data obtained from the tower. From 40 samples nineteen runs were found, satisfying the $\alpha = 0.05$ level of significance set down by Bendat and Piersol (ref 1). This 468 second sample was the only data found which exhibited such stationarity in wind excited structural response over a significant time frame. Having effectively removed the forcing (wind) non-stationarity from the data, what remains is the non-linear response of the tower itself.

The stationary set of data was then bandpass filtered at the first mode and an autocorrelation analysis performed. The resulting autocorrelation curves shown in Figure8 indicate that damping along both tower axes is of similar magnitude at low amplitudes. Both levels of damping are typical for a steel structure under serviceability stress levels (ref5).

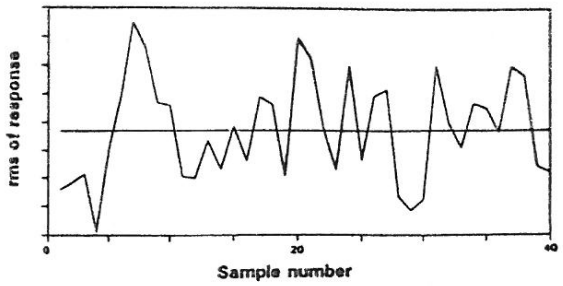

Figure 7 Run test for stationarity using 40 samples

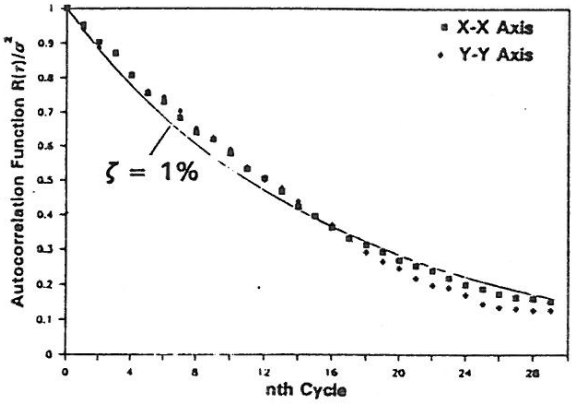

Figure 8 Autocorrelation function of first mode acceleration.

4.2 Wind Induced Response

A time history of tower acceleration and wind velocity over a 40 second period is shown in Figure9. Mode one is seen to dominate while modes two and three contribute towards the background response of the tower. An increase in along wind (Y-Y) response can be seen due to wind energy fluctuating near n_1 between 20 and 40 seconds. A locus of dynamic response over 50 seconds is shown in Figure10. Along-wind and cross-wind components are of similar magnitude due to the strong coupling which exists between the two axes.

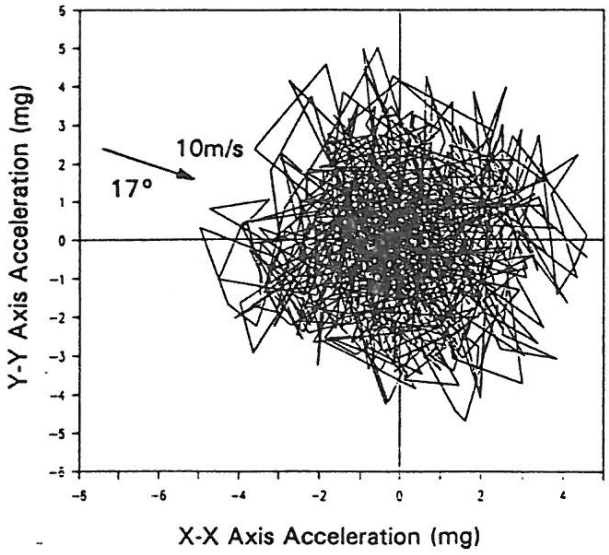

Figure 10 Locus of tower acceleration

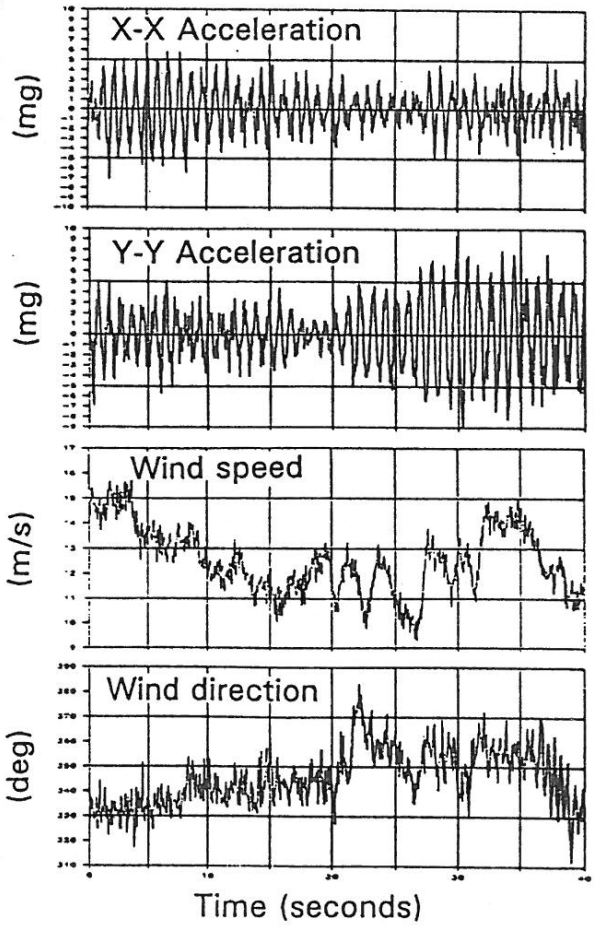

Figure 9 Time history of tower acceleration, wind speed and direction

Figure11 show that rms acceleration increases in proportion to the square of wind velocity for both along-wind and cross-wind components. Full scale measurements completed by Hiramatsu and Akagi (ref2) on more conventional angular section tower's of similar height to the Prospect tower indicate that tower response increases as a power of 2.5. The long records (819 seconds) exhibit less scatter than the short records (63 seconds) due to smaller statistical errors. Variation in turbulence also contributes to the scatter shown in Figure11.

Fluctuation in wind speed is plotted against the dynamic response of the tower in cross-wind and along-wind direction in Figure12. There is a general increase in tower response with increasing gust.

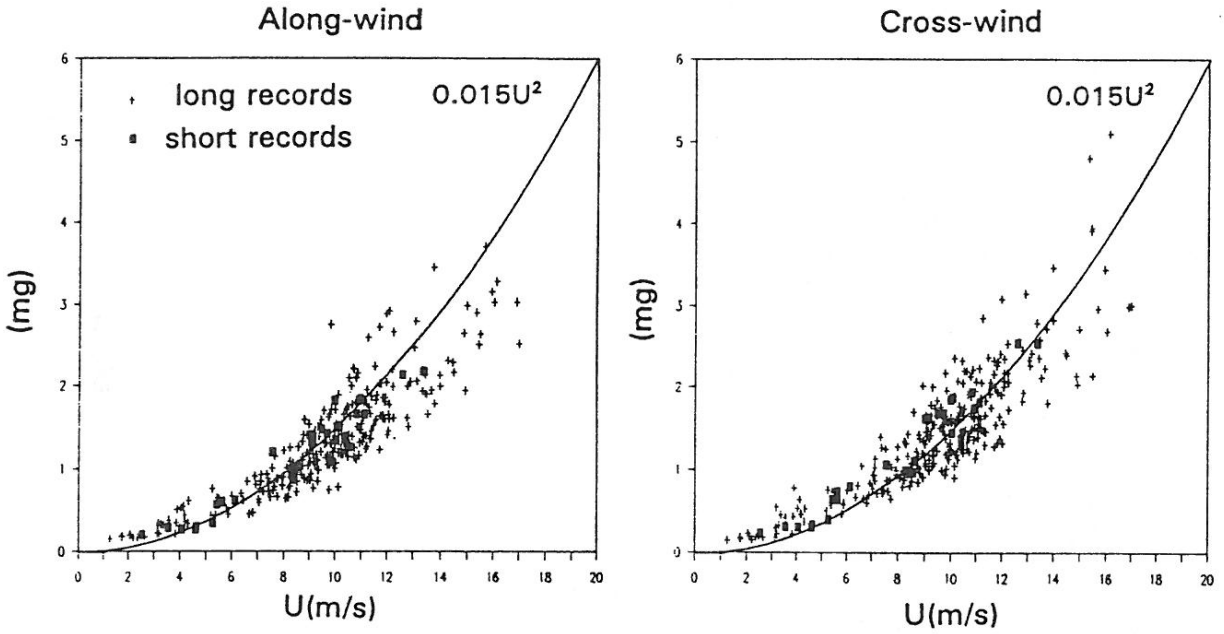

Figure 11 rms acceleration versus mean wind speed

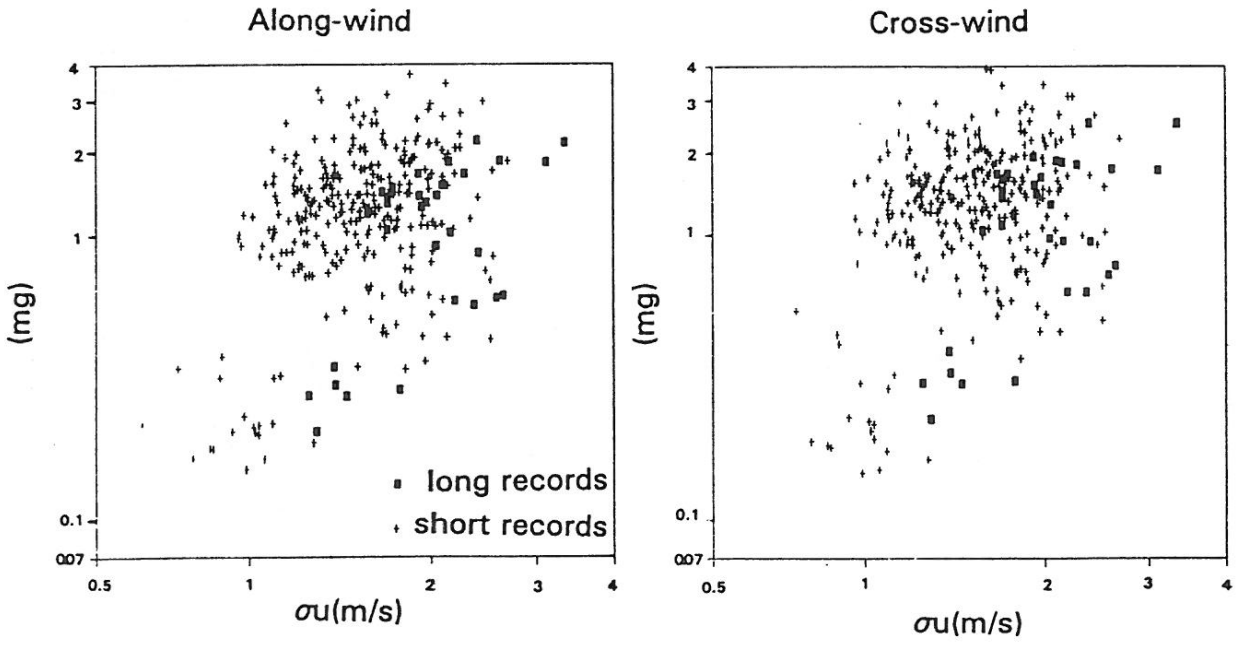

Figure 12 rms acceleration versus wind speed fluctuation

Figure13 shows that turbulence ($\sigma v/U$) decreases with increasing mean wind speed up to about 8m/s. At this point $\sigma v/U$ levels off to about 0.151 (the value assumed by AS1170.2 for terrain category 2 at 50m). It is suspected that high turbulence at low wind speed is partly due to the inertia of the anemometer cups.

Mean wind speed is plotted against peak factor g (ratio of maximum and standard deviation) in Figure14. This measured peak factor represents a single maxima found in the signal over a period T. Peak factor g increases with increasing averaging time T although there is no change with increasing mean wind speed. Davenport has derived an 'average' peak factor g_R for resonant response based on a narrow band Gaussian process according to the equation.

$$g_R = \sqrt{2\log_e(n_1 T)} + \gamma/\sqrt{2\log_e(n_1 T)}$$

γ is Euler's constant equal to 0.5772 whilst n_1 is the first natural frequency of the tower. Expected peak g_R is plotted in Figure14 and is seen to be lower than the absolute peak g measured as would be expected.

Acceleration due to tilting of the tower has not been separated from the resonant response accelerations since its contribution is negligible.

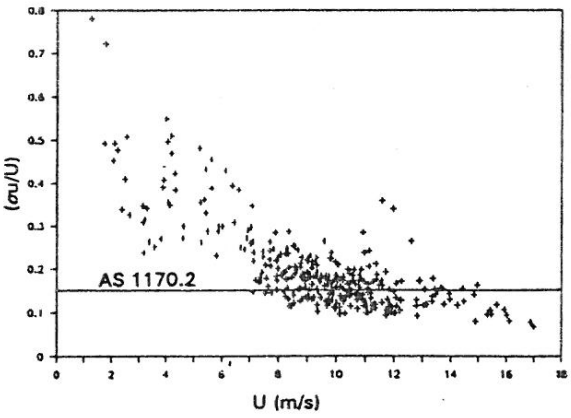

Figure 13 Turbulence intensity versus mean wind speed

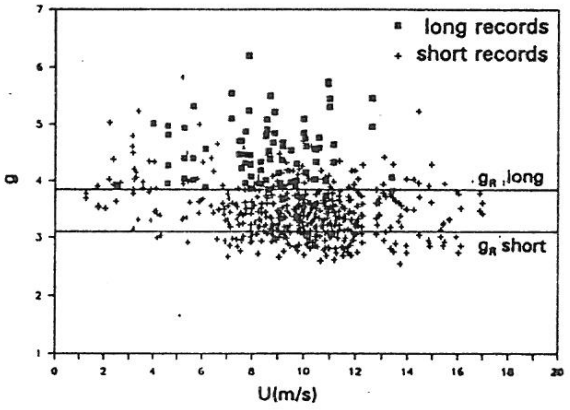

Figure 14 Peak factor versus mean wind speed

5. Conclusions

Natural frequencies and mode shapes of the Prospect tower are measured in full scale and agree well with a STRAND6 computer prediction. Mode one dominates the response of the tower at 1.08Hz whilst mode two represents vibration of the top mast on the tower alone. Damping is determined by large amplitude (5-170mg) free vibration decay and low amplitude (<5mg) autocorrelation analysis. Damping for the tower is around 1% critical damping for mode one. The along wind and cross wind response of the tower was found to increase in proportion to the square of mean wind speed which is lower than the response expected from more conventional angle section towers of similar height. A clear correlation is found between increasing fluctuation of wind speed and increasing tower response.

References:

1. Bendat,J Piersol,A: 'Measurement and analysis of random data',J Wiley,New York,1966
2 Hiramatsu,K Akagi,H: 'The response of latticed steel towers due to the action of wind',Journal of Wind Engineering and industrial Aerodynamics, 30 (1988) 7-16.
3 Holmes,J.D.: 'Along-wind response of lattice towers' personal communication
4 Jeary,A.P.: 'Establishing non-linear damping characteristics of structures from non-stationary response time histories',The Structural Engineer/Volume 70/No.4/18 February 1992
5 Standards Australia. AS1170.2-1989'SAA loading code. Part2: Wind Loads',Standards Australia,North Sydney,1989